



Title	Two-mode PLC-based mode multi/demultiplexer for mode and wavelength division multiplexed transmission
Author(s)	Hanzawa, Nobutomo; Saitoh, Kunimasa; Sakamoto, Taiji; Matsui, Takashi; Tsujikawa, Kyojo; Koshiba, Masanori; Yamamoto, Fumihiko
Citation	Optics express, 21(22), 25752-25760 https://doi.org/10.1364/OE.21.025752
Issue Date	2013-11-04
Doc URL	http://hdl.handle.net/2115/54602
Rights	This paper was published in Optics Express and is made available as an electronic reprint with the permission of OSA. The paper can be found at the following URL on the OSA website: http://www.opticsinfobase.org/oe/abstract.cfm?uri=oe-21-22-25752 . Systematic or multiple reproduction or distribution to multiple locations via electronic or other means is prohibited and is subject to penalties under law.
Type	article
File Information	oe-21-22-25752.pdf



[Instructions for use](#)

Two-mode PLC-based mode multi/demultiplexer for mode and wavelength division multiplexed transmission

Nobutomo Hanzawa,^{1,*} Kuimasa Saitoh,² Taiji Sakamoto,¹ Takashi Matsui,¹ Kyozo Tsujikawa,¹ Masanori Koshiba,² and Fumihiko Yamamoto¹

¹ NTT Access Network Service Systems Laboratories, NTT Corporation, Hanabatake 1-7-1, Tsukuba, Ibaraki, 305-0805, Japan

² Graduate School of Information Science and Technology, Hokkaido University, Sapporo, 060-0814, Japan
hanzawa.nobutomo@lab.ntt.co.jp

Abstract: We proposed a PLC-based mode multi/demultiplexer (MUX/DEMUX) with an asymmetric parallel waveguide for mode division multiplexed (MDM) transmission. The mode MUX/DEMUX including a mode conversion function with an asymmetric parallel waveguide can be realized by matching the effective indices of the LP₀₁ and LP₁₁ modes of two waveguides. We report the design of a mode MUX/DEMUX that can support C-band WDM-MDM transmission. The fabricated mode MUX/DEMUX realized a low insertion loss of less than 1.3 dB and high a mode extinction ratio that exceeded 15 dB. We used the fabricated mode MUX/DEMUX to achieve a successful 2 mode x 4 wavelength x 10 Gbps transmission over a 9 km two-mode fiber with a penalty of less than 1 dB.

©2013 Optical Society of America

OCIS codes: (060.2270) Fiber characterization; (060.2400) Fiber properties.

References and links

1. D. Qian, M. F. Huang, E. Ip, Y. K. Huang, Y. Shao, J. Hu, and T. Wang, "101.7-Tb/s (370x294-Gb/s) PDM-128QAM-OFDM transmission over 3x55-km SSMF using pilot-based phase noise mitigation," OFC2011, paper PDPB5 (2011).
2. T. Morioka, Y. Awaji, R. Ryf, P. Winzer, D. Richardson, and F. Poletti, "Enhancing optical communications with brand new fibers," IEEE Commun. Mag. **50**(2), s31–s42 (2012).
3. K. Imamura, Y. Tsuchida, K. Mukasa, R. Sugizaki, K. Saitoh, and M. Koshiba, "Investigation on multi-core fibers with large Aeff and low micro bending loss," Opt. Express **19**(11), 10595–10603 (2011).
4. T. Hayashi, T. Taru, O. Shimakawa, T. Sasaki, and E. Sasaoka, "Characterization of crosstalk in ultra-low-crosstalk multi-core fiber," J. Lightwave Technol. **30**(4), 583–589 (2012).
5. M. Koshiba, K. Saitoh, K. Takenaga, and S. Matsuo, "Analytical expression of average power-coupling coefficients for estimating intercore crosstalk in multicore fibers," IEEE Photon. J. **4**(5), 1987–1995 (2012).
6. K. Saitoh, M. Koshiba, K. Takenaga, and S. Matsuo, "Crosstalk and core density in uncoupled multicore fibers," IEEE Photon. Technol. Lett. **24**(21), 1898–1901 (2012).
7. H. Takara, A. Sano, T. Kobayashi, H. Kubota, H. Kawakami, A. Matsuura, Y. Miyamoto, Y. Abe, H. Ono, K. Shikama, Y. Goto, K. Tsujikawa, Y. Sasaki, I. Ishida, K. Takenaga, S. Matsuo, K. Saitoh, M. Koshiba, and T. Morioka, "1.01-Pb/s(12 SDM/222 WDM/456 Gb/s) crosstalk-managed transmission with 91.4-b/s/Hz aggregate spectral efficiency," ECOC2012, paper Th.3.C.1 (2012).
8. V. A. J. M. Sleiffer, Y. Jung, V. Veljanovski, R. G. H. van Uden, M. Kuschnerov, H. Chen, B. Inan, L. G. Nielsen, Y. Sun, D. J. Richardson, S. U. Alam, F. Poletti, J. K. Sahu, A. Dhar, A. M. J. Koonen, B. Corbett, R. Winfield, A. D. Ellis, and H. de Waardt, "73.7 Tb/s (96 x 3 x 256-Gb/s) mode-division-multiplexed DP-16QAM transmission with inline MM-EDFA," Opt. Express **20**(26), B428–B438 (2012).
9. E. Ip, N. Bai, Y. K. Huang, E. Mateo, F. Yaman, M. J. Li, S. Bickham, S. Ten, J. Liñares, C. Montero, V. Moreno, X. Prieto, V. Tse, K. M. Chung, A. Lau, H. Y. Tam, C. Lu, Y. Luo, G. D. Peng, and G. Li, "88x3x112-Gb/s WDM transmission over 50 km of three-mode fiber with inline few-mode fiber amplifier," ECOC2011, paper Th.13.C.2 (2011).
10. N. Hanzawa, K. Saitoh, T. Sakamoto, T. Matsui, S. Tomita, and M. Koshiba, "Asymmetric parallel waveguide with mode conversion for mode and wavelength division multiplexing transmission," OFC2012, paper OTU11.4 (2012).
11. R. Ryf, R. Essiambre, A. H. Gnauck, S. Randel, M. A. Mestre, C. Schmidt, P. J. Winzer, R. Delbue, P. Pupalaiakis, A. Sureka, T. Hayashi, T. Taru, and T. Sasaki, "Space-division multiplexed transmission over 4200-km 3-Core microstructured fiber," OFC2012, paper PDP5C.2 (2012).

12. A. Li, X. Chen, A. Al Amin, and W. Shieh, "Fused fiber mode couplers for few-mode transmission," *IEEE Photon. Technol. Lett.* **24**(21), 1953–1956 (2012).
13. R. Ryf, N. K. Fontaine, and R. Essiambre, "Spot-based mode couplers for mode-multiplexed transmission in few-mode fiber," *IEEE Photon. Technol. Lett.* **24**(21), 1973–1976 (2012).
14. T. Sakamoto, T. Mori, T. Yamamoto, and S. Tomita, "Differential mode delay managed transmission line for WDM-MIMO system using multi-step Index fiber," *J. Lightwave Technol.* **30**(17), 2783–2787 (2012).
15. T. Mori, T. Sakamoto, M. Wada, T. Yamamoto, and F. Yamamoto, "Low DMD four LP mode transmission fiber for wide-band WDM-MIMO system," OFC2013, paper OTh3K.1 (2013).
16. R. Ryf, M. A. Mestre, A. H. Gnauck, S. Randel, C. Schmidt, R.-J. Essiambre, P. J. Winzer, R. Delbue, P. Pupalaikis, A. Sureka, Y. Sun, X. Jiang, D. W. Peckham, A. McCurdy, and R. Lingle, Jr., "Low-loss mode coupler for mode-multiplexed transmission in few-mode fiber," OFC2012, paper PDP5B.5 (2012).
17. R. Ryf, S. Randel, N. K. Fontaine, M. Montoliu, E. Burrows, S. Corteselli, S. Chandrasekhar, A. H. Gnauck, C. Xie, R.-J. Essiambre, P. J. Winzer, R. Delbue, P. Pupalaikis, A. Sureka, Y. Sun, L. Gruner-Nielsen, R. V. Jensen, and R. Lingle, Jr., "32-bit/s/Hz spectral efficiency WDM transmission over 177-km few-mode fiber," OFC2013, paper PDP5A.1 (2013).
18. N. K. Fontaine, R. Ryf, B. Guan, and D. T. Neilson, "Wavelength blocker for few-mode-fiber space-division multiplexed systems," OFC2013, paper OTh1B.1 (2013).
19. T. Uematsu, K. Saitoh, N. Hanzawa, T. Sakamoto, T. Matsui, K. Tsujikawa, and M. Koshiha, "Low-loss and broadband PLC-type mode (de)multiplexer for mode-division multiplexing transmission," OFC2013, paper OTh1B.5 (2013).
20. M. Oguma, T. Kitoh, A. Mori, and H. Takahashi, "Ultrawide-passband tandem MZI-synchronized AWG and group delay ripple balancing out technique," ECOC2010, paper We8.E.2 (2010).
21. H. Kubota, M. Oguma, and H. Takara, "Three-mode multi/demultiplexing experiment using PLC mode multiplexer and its application to 2+1 mode bi-directional optical communication," *IEICE Electron. Express* **10**(12), 1–6 (2013).
22. W. V. Sorin, B. Y. Kim, and H. J. Shaw, "Highly selective evanescent modal filter for two-mode optical fibers," *Opt. Lett.* **11**(9), 581–583 (1986).

1. Introduction

The network traffic in optical fiber communication systems has increased rapidly. Although a transmission capacity of more than 100 Tbps has been realized by using dense WDM and a multi-level modulation format in standard single-mode fiber (SMF) [1], exceeding this capacity is considered to be difficult with these technologies because of the input power limitation caused by the nonlinear effect. Therefore new technologies including space-division multiplexing (SDM) and mode-division multiplexing (MDM) have received increasing attention with the aim of realizing a much larger capacity [2]. A multi-core fiber has been studied with a view to greatly increasing transmission capacity [3–6], and a transmission exceeding 1 Pbps has been realized by using 12-core fiber [7].

As regards MDM transmission, a transmission capacity exceeding 70 Tbps has been realized by using two LP modes with a few-mode fiber [8]. Various types of mode multi/demultiplexer (MUX/DEMUX) and few-mode fiber have been proposed [9–19]. Of the proposed mode MUX/DEMUXs, the free-space optics based mode MUX/DEMUX encountered a difficulty in terms of reducing the insertion loss because a half-mirror was used for mode multi/demultiplexing [8,9]. Although a mode MUX/DEMUX using free-space optics with a low insertion loss has been proposed [16–18], the setup requires precise alignment. Thus, a number of problems must be overcome if the free-space optics based mode MUX/DEMUX is to realize a low insertion loss. PLC-based devices offer the advantages of compactness, low loss and mass-producibility because of their mature manufacturing technology. The PLC-based mode converter with multimode waveguide has been proposed for broad-band MUX/DEMUX in WDM transmission [20]. Recently, several PLC-based mode MUX/DEMUXs have been proposed in order to realize MDM transmission [10,19,21].

In this paper, we show that we can realize an asymmetric mode coupler (AMC) as a mode MUX/DEMUX by matching the effective indices of the LP_{01} and LP_{11} modes of two waveguides. We investigated the relationship between the LP_{01} to LP_{11} mode coupling ratio and the bandwidth as regards the waveguide parameters of the AMC. We then fabricated an AMC supporting C-band MDM-WDM transmission, which realized a low insertion loss of less than 1.3 dB and a high mode extinction ratio of more than 15 dB. Finally, we achieved an MDM-WDM transmission in the C-band over a 9 km-long two-mode fiber with a low power penalty of less than 1 dB by using the fabricated AMC.

2. Mode multi/demultiplexing with asymmetric mode coupler

Figure 1 is a diagram of the basic AMC. The AMC has two waveguides with widths of w_1 and w_2 ($w_1 > w_2$) as shown in Fig. 1(a). A cross-section of the waveguide is also shown in Fig. 1(b). Here, G , L and h are the waveguide gap, interaction length and waveguide height, respectively, and h is the same as w_2 . The LP_{01} mode from port 2 is converted to the LP_{11} mode in waveguide 1 and output at port 3, and the LP_{01} mode from port 1 is output directly at port 3. Thus, the LP_{01} and LP_{11} modes are multiplexed at port 3. The AMC can also be used as a mode DEMUX because the coupler has a symmetric property. Since the input or output signals at a MUX/DEMUX are propagated as the fundamental mode when we use this AMC, we can construct an MDM transmission system with conventional single-mode optical devices in transmitters and receivers.

The mode coupling between the LP_{01} and LP_{11} modes needs to match the effective index of the LP_{11} mode in waveguide 1 to that of the LP_{01} mode in waveguide 2 as shown in Fig. 2(a) [20]. The effective indices of the LP_{01} and LP_{11} modes increase with the waveguide width when the relative refractive index difference (Δ) is constant. Thus, the LP_{01} mode in waveguide 2 can be coupled to the LP_{11} mode in waveguide 1 by increasing w_1 appropriately compared with w_2 as shown in Fig. 2(a). Figure 2(b) shows the waveguide width dependence of the effective indices of the LP_{01} and LP_{11} modes at a wavelength of 1550 nm. Here, we assumed that Δ was 0.4% and the waveguide height and width were the same. Since single-mode operation can be realized with a waveguide width smaller than $7.5 \mu\text{m}$ over the S – L bands with this Δ , we selected a w_2 value of $7.5 \mu\text{m}$. To match the effective indices of the LP_{11} and LP_{01} modes, the w_1 and w_2 values were required to be $19.3 \mu\text{m}$ and $7.5 \mu\text{m}$, respectively. So the mode multi/demultiplexing of the LP_{01} and LP_{11} modes can be realized with an appropriate L on a certain G for these waveguide widths.

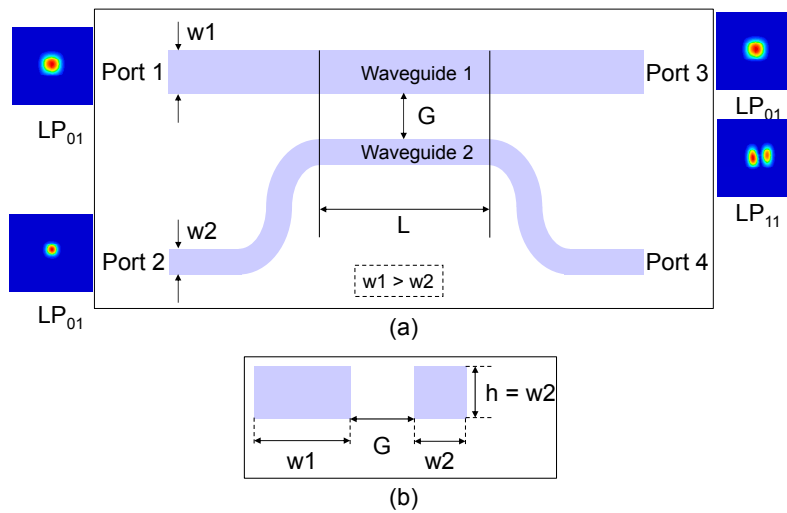


Fig. 1. Basic concept of AMC with mode conversion. (a) Overhead view. (b) Cross-section view.

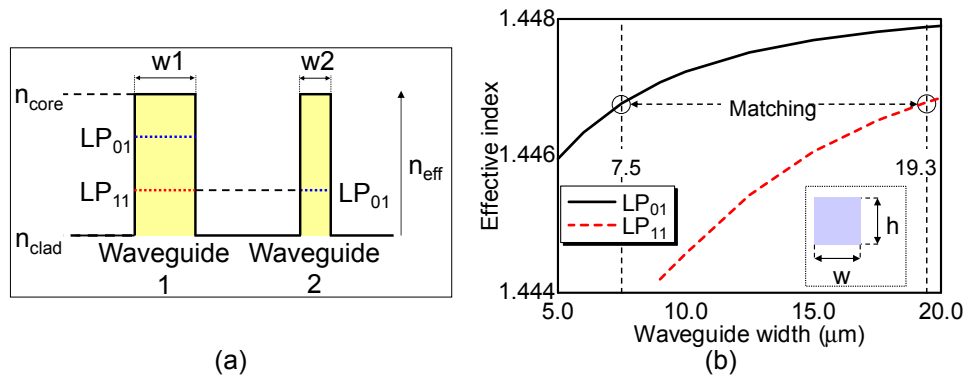


Fig. 2. (a) Image of effective index for mode coupling between LP_{01} and LP_{11} modes. (b) Waveguide width dependence of effective index.

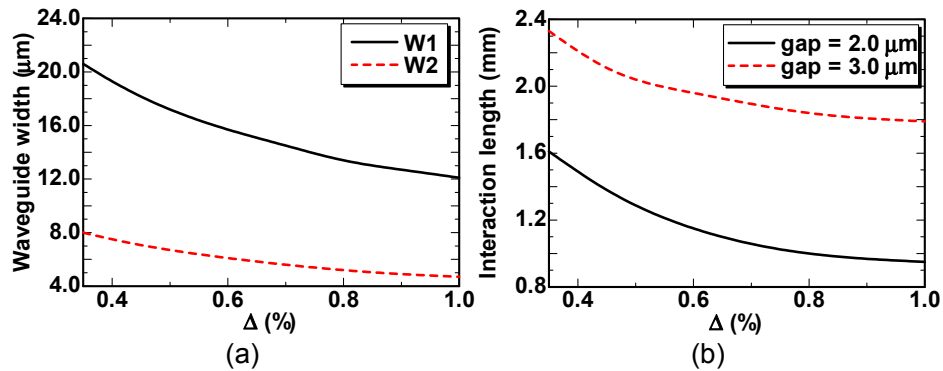


Fig. 3. (a) Waveguide width dependence of Δ . (b) Interaction length dependence of Δ .

Figures 3(a) and 3(b) show the Δ dependence of the waveguide width and interaction length for realizing the maximum mode coupling efficiency between the LP_{01} and LP_{11} modes. The solid and dashed lines show waveguide widths w_1 and w_2 , respectively. w_2 was set at the maximum value for single-mode operation at a wavelength of 1450 nm when we assumed a square waveguide structure. w_1 was about 2.6 times as wide as w_2 with the same height as shown Fig. 3(a). We then calculated the interaction length as the peak coupling ratio of the LP_{11} mode at a wavelength of 1550 nm for each Δ when we set the gaps at 2.0 and 3.0 μm , respectively. The solid and dashed lines show the interaction length in gaps for 2.0 and 3.0 μm , respectively. The interaction length became long as the waveguide gap increased as shown in Fig. 3(b). Moreover, the interaction length remained constant with increasing Δ .

We designed the AMC with a Δ of 0.4%, a w_1 of 19.3 μm , and a w_2 of 7.5 μm . Although the AMC can use degenerate modes (LP_{11a} and LP_{11b}), we assumed the use of only the LP_{11a} mode in this design. Figure 4 shows the interaction length calculated as a function of G . Here, L was calculated as the peak coupling ratio of the LP_{11} mode at a wavelength of 1550 nm. L was roughly proportional to G . When we set G values of 3.0 and 4.0 μm , the L values were 2.21 and 3.31 mm, respectively. Figures 5(a) and 5(b) show the wavelength dependence of the coupling ratio to port 3 from ports 1 and 2 as a function of wavelength for G values of 3.0 and 4.0 μm , respectively. The solid, dashed and dotted lines show the coupling ratios of the LP_{01} , LP_{11x} , and LP_{11y} modes, respectively. Here, the coupling ratio of the LP_{01} mode indicated the x-polarized value because the coupling ratios of the x and y polarizations in the LP_{01} mode were almost the same. The coupling ratio of the LP_{01} mode was higher than 98% at gaps of 3.0 and 4.0 μm between 1450 ~1650 nm. The coupling ratios of the LP_{01} and LP_{11} modes were higher than 98% at gaps of 3.0 and 4.0 μm in the entire C-band. Moreover, we consider

that this AMC could be used in an MDM system with polarization division multiplexing because of its low polarization dependence.

We then calculated the peak coupling ratio and the bandwidth for 1% down from the peak coupling ratio. Figure 6 shows the peak coupling ratio and bandwidth as a function of the waveguide gap. The solid and dashed lines show the x and y polarizations in the LP₁₁ mode. Here, the coupling ratio of the LP₀₁ mode was almost 100% at a gap of more than 4.0 μm. There were relatively large changes in the coupling ratio and bandwidth with gaps between 2.0 and 3.0 μm. Then the coupling ratio increased monotonously with gaps between 3.0 and 6.0 μm. In contrast, the bandwidth decreased as the waveguide gap increased. So the peak coupling ratio and bandwidth had a tradeoff relation, and these values were polarization insensitive. Therefore, we assumed that a relatively high coupling ratio and wide bandwidth can be realized by adopting a gap of between 3.0 and 4.0 μm in the AMC.

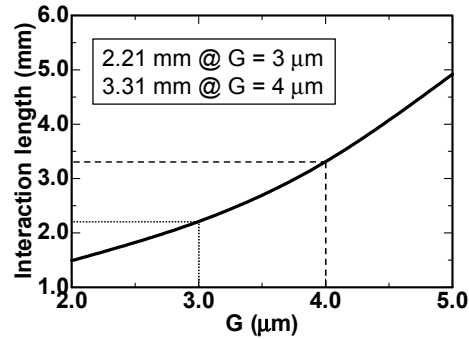


Fig. 4. Interaction length dependence on waveguide gap.

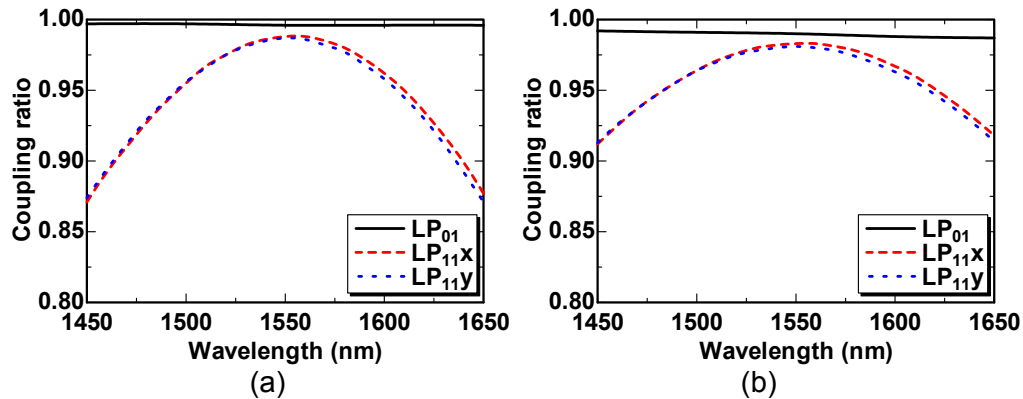


Fig. 5. (a) Coupling ratio dependence wavelength with 3.0 μm gap. (b) Coupling ratio dependence wavelength with 4.0 μm gap.

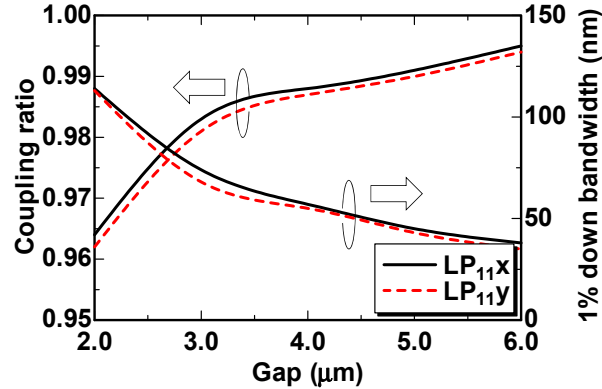


Fig. 6. Peak coupling ratio and 1% down bandwidth from peak coupling ratio dependences of gap.

3. Property of fabricated AMC

We then fabricated two kinds of AMC with our design parameters as shown in Table 1. Here, two-mode fibers with a core diameter of $14.0\ \mu\text{m}$ were connected to the ends of ports 1 and 3 in the fabricated AMC. AMC1 and AMC2 had the same waveguide width. First, we investigated the mode conversion performance. Figure 7 shows the near field patterns (NFPs) measured at the output port at a wavelength of $1550\ \text{nm}$. The first and second rows in Fig. 7 were NEPs in AMC1 and AMC2, respectively. The first, second, and third columns were the NFPs when CW light was input into ports 1 or 2 and both ports, respectively. The LP_{01} mode pattern was observed at port 3 when input into port 1. The LP_{11} mode pattern was clearly observed by converting the LP_{01} mode from port 2 to the LP_{11} mode in the waveguides. We also observed a mixed electric field consisting of the LP_{01} and LP_{11} modes when CW light was input into both ports. We also observed similar field patterns for AMC2 as shown in the second row of Fig. 7. Thus the fabricated AMCs successfully performed as a mode multiplexer for the LP_{01} and LP_{11} modes.

We measured the insertion losses of the LP_{01} and LP_{11} modes between 1500 and $1620\ \text{nm}$. Figures 8(a) and 8(b) show the insertion losses of AMC1 and AMC2, respectively. The open and filled circles are the insertion losses of the LP_{01} and LP_{11} modes, respectively. The insertion loss of the fabricated AMCs had a low wavelength dependence and the insertion losses of AMC1 and AMC2 were less than 0.8 and $1.3\ \text{dB}$, respectively. We considered the insertion loss of AMC2 to be larger than that of AMC1 because with AMC2 there was a misalignment between the waveguide and the splicing fiber. We realized a low insertion loss with a low mode dependence. Since the primary factor as regards the insertion loss was the mode field diameter (MFD) mismatch between the waveguide and the splicing fiber, we believe that the insertion loss can be improved by reducing the MFD mismatch.

The measured mode extinction ratios of AMC1 and AMC2 are shown in Figs. 9(a) and 9(b), respectively. The open and filled circles show the LP_{11} to LP_{01} and LP_{01} to LP_{11} mode extinction ratios, respectively. Additionally, the solid and dashed lines are the calculated LP_{01} to LP_{11} and LP_{11} to LP_{01} mode extinction ratios, respectively. We confirmed that the calculated result agreed relatively well with the measured result. The LP_{01} to LP_{11} mode extinction ratio exceeded $20\ \text{dB}$ between 1500 and $1620\ \text{nm}$ in both fabricated AMCs. Furthermore, the LP_{11} to LP_{01} mode extinction ratio exceeded $15\ \text{dB}$ over the C-band. Therefore, we were able to realize a mode MUX/DEMUX with a low insertion loss and a relatively high mode extinction ratio. In the future, we believe that a higher mode extinction ratio and wider bandwidth will be realized by employing the WINC structure [19].

Table 1. Waveguide parameters of fabricated AMC

	w1 (μm)	w2 (μm)	G (μm)	L (mm)	Δ (%)
AMC1	19.3	7.5	3.0	2.21	0.4
AMC2	19.3	7.5	4.0	3.31	0.4

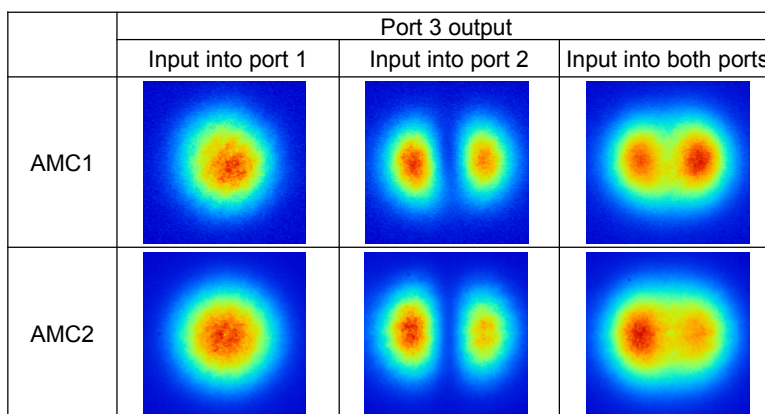


Fig. 7. Near field patterns of AMC1 and AMC2.

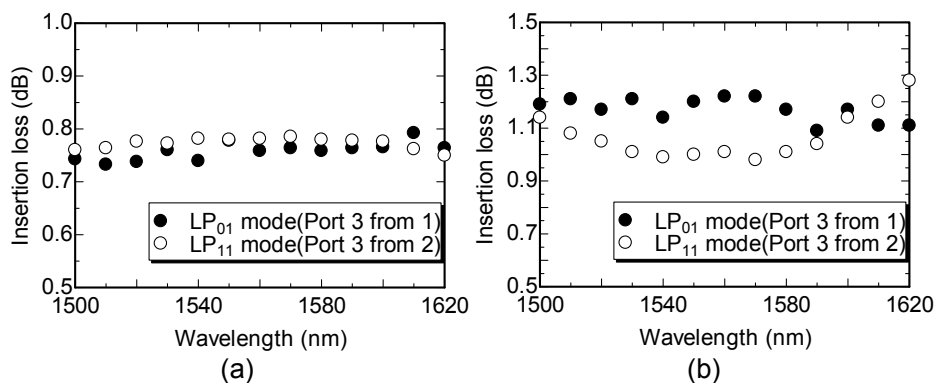


Fig. 8. (a) Wavelength dependence of insertion loss in AMC1. (b) Wavelength dependence of insertion loss in AMC2.

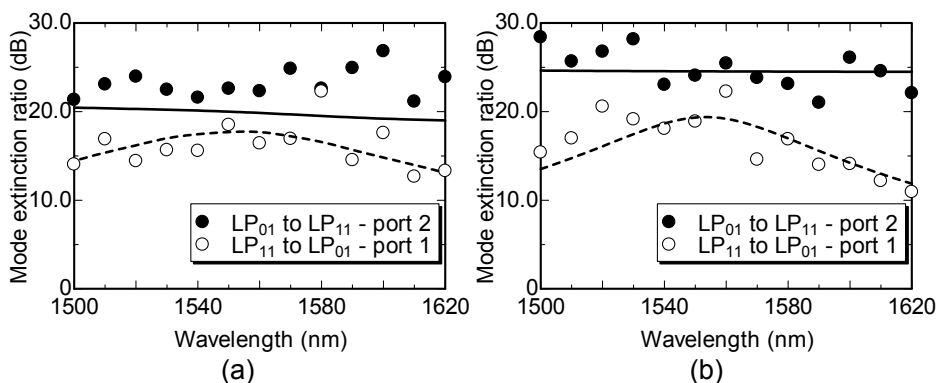


Fig. 9. (a) Wavelength dependence of mode extinction ratio in AMC1. (b) Wavelength dependence of mode extinction ratio in AMC2.

4. Mode division multiplexed transmission with fabricated AMC

We constructed the MDM transmission setup shown in Fig. 10. As a transmission medium we used a two-mode 9 km-long step-index fiber with an effective cut-off wavelength for the LP_{11} mode of longer than 1600 nm. The MFD and the transmission loss of the LP_{01} mode were 11.69 μm and 0.2 dB/km, respectively, at a wavelength of 1550 nm. The light sources were DFB-LDs operating at 1534, 1542, 1552, and 1557 nm. These lights were modulated at 10 Gbps in a non-return-to-zero modulation format with a $2^{31}-1$ pseudorandom binary sequence (PRBS) by using a lithium niobate (LN) intensity modulator. The optical signals were divided into two with a 3 dB power coupler and guided into ports 1 and 2, respectively in the mode MUX. Signals at port 1 were guided into a transmission medium in the LP_{01} mode via the designed mode MUX. In contrast, the signals at port 2 were multiplexed in the LP_{11} mode in the transmission medium after the LP_{01} modes had been converted to LP_{11} modes in the mode MUX. These transmitted MDM-WDM signals were demultiplexed with a mode DEMUX, which had the same structure as the mode MUX, and were then demultiplexed to each wavelength with an AWG. After that each channel was amplified with an erbium-doped fiber amplifier (EDFA). Figures 11(a) and 11(b), respectively, show the BER characteristics as a function of the received power of the LP_{01} and LP_{11} modes with AMC1. Figures 11(c) and 11(d), respectively, show the BERs of the LP_{01} and LP_{11} modes with AMC2. The solid and dashed lines show the BERs for back-to-back and 9 km transmissions, respectively. We confirmed that the LP_{01} and LP_{11} modes were successfully transmitted without any noticeable error floor.

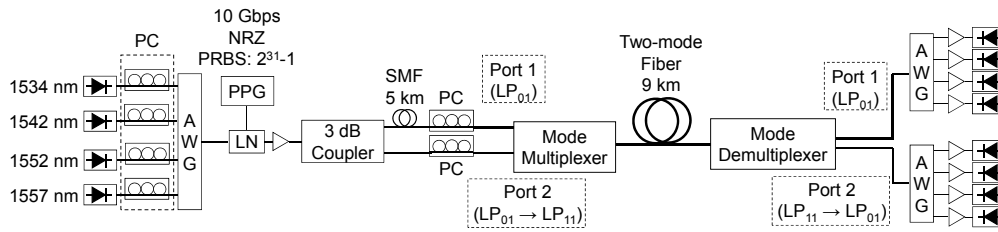


Fig. 10. Experimental setup for MDM-WDM transmission.

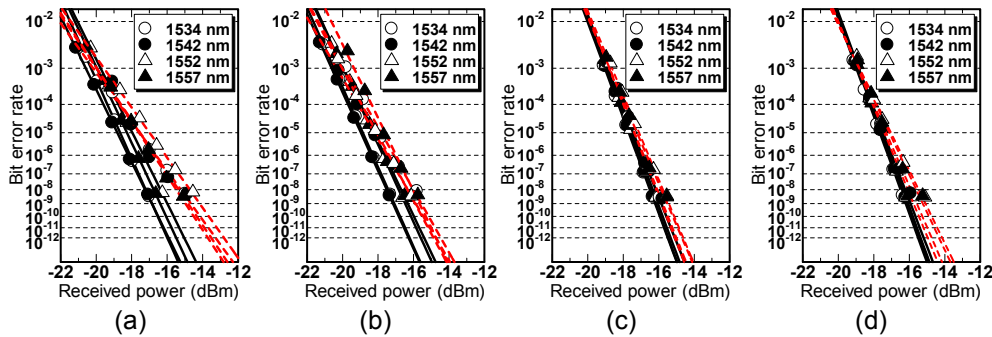


Fig. 11. MDM-WDM BER characteristics. (a) LP_{01} mode transmission with AMC1. (b) LP_{11} mode transmission with AMC1. (c) LP_{01} mode transmission with AMC2. (d) LP_{11} mode transmission with AMC2.

The penalty of the LP_{01} mode transmission was larger than that for the LP_{11} mode with AMC1 as shown in Figs. 11(a) and 11(b). We assumed that this penalty was generated by the LP_{11b} mode crosstalk. The LP_{11b} mode was insufficiently suppressed because of the short interaction length in AMC1. The LP_{01} and LP_{11} modes were successfully transmitted with a power penalty of less than 1 dB by using AMC2, which has a longer interaction length than AMC1. Although the LP_{11b} mode suppression was effective in increasing the interaction length, a long interaction length had a reduced bandwidth as shown in Fig. 6. Therefore, when designing an AMC we must consider the coupling ratio, bandwidth and suppression of unnecessary modes in order to satisfy the MDM transmission characteristics. Our results show that the PLC-based mode MUX/DEMUX can contribute to MDM-WDM transmission.

5. Conclusion

We proposed a mode multi/demultiplexer (MUX/DEMUX) with an asymmetric mode coupler (AMC) for mode division multiplexed (MDM) transmission, and we designed its waveguide parameters. Our calculation results show that the coupling ratio and bandwidth had a tradeoff relationship. We realized mode multiplexing/demultiplexing with an AMC that we designed and fabricated with waveguide parameters for multiplexing the LP_{01} and LP_{11} modes. A 2 mode x 4 wavelength x 10 Gbps MDM-WDM transmission was successfully realized over a 9 km-long two-mode fiber in the C-band with a low-power penalty.

Acknowledgments

We thank S. Tomita for his support and fruitful discussions.